

http://www.chxb.cn
ISSN 0253-9837
CN 21-1195/O6
CODEN THHPD3

催化学报

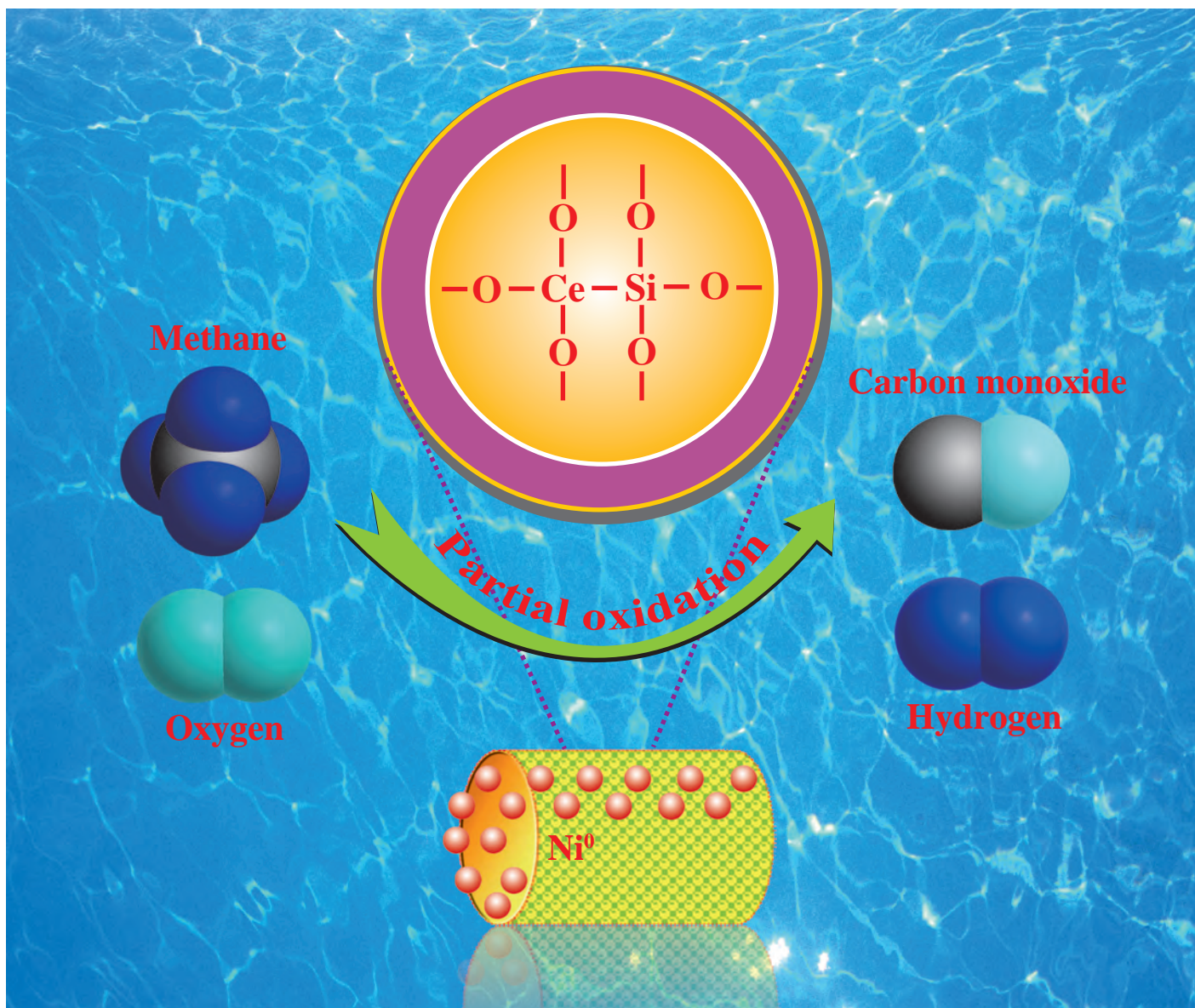
Chinese Journal of Catalysis

主编 林励吾

Editor-in-Chief LIN Liwu

2014

Vol. 35 No. 1



ISSN 0253-9837

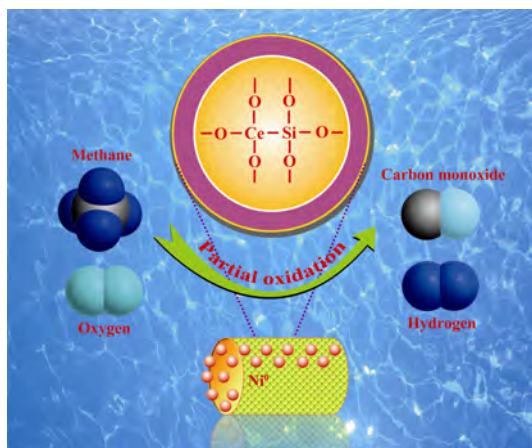


9 770253 983146

中国化学会催化学会会刊

Transaction of the Catalysis Society of China

In This Issue



封面: 胡久彪等报道了溶胶-凝胶法合成大比表面积的 CeO₂-SiO₂ 复合氧化物, 其负载 Ni 后, Ni 与载体的化学作用较弱, NiO 的分散性良好, 酸性弱, 催化性能优异, 且稳定性较高. 见本期第 8-20 页.

Cover: Hu and coworkers in their Article on pages 8-20 reported that CeO₂-SiO₂ composite oxides with large surface area synthesized using a sol-gel process. The nickel catalyst supported on the as-synthesized CeO₂-SiO₂ had good properties and stability, which resulted from the weak chemical interaction between Ni and support, good dispersion of NiO, weak acidity, and low carbon deposition.

About the Journal

Chinese Journal of Catalysis is an international journal published monthly by Chinese Chemical Society, Dalian Institute of Chemical Physics, Chinese Academy of Sciences, and Elsevier. The journal publishes original, rigorous, and scholarly contributions in the fields of heterogeneous and homogeneous catalysis in English or in both English and Chinese. The scope of the journal includes:

- ◆ New trends in catalysis for applications in energy production, environmental protection, and production of new materials, petroleum chemicals, and fine chemicals;
 - ◆ Scientific foundation for the preparation and activation of catalysts of commercial interest or their representative models;
 - ◆ Spectroscopic methods for structural characterization, especially methods for in situ characterization;
 - ◆ New theoretical methods of potential practical interest and impact in the science and applications of catalysis and catalytic reaction;
 - ◆ Relationship between homogeneous and heterogeneous catalysis;
 - ◆ Theoretical studies on the structure and reactivity of catalysts.
- ◆ The journal also accepts contributions dealing with photo-catalysis, bio-catalysis, and surface science and chemical kinetics issues related to catalysis.

Types of Contributions

- **Reviews** deal with topics of current interest in the areas covered by this journal. Reviews are surveys, with entire, systematic, and important information, of recent progress in important topics of catalysis. Rather than an assemblage of detailed information or a complete literature survey, a critically selected treatment of the material is desired. Unsolved problems and possible developments should also be discussed. Authors should have published articles in the field. Reviews should have more than 80 references.
- **Communications** rapidly report studies with significant innovation and major academic value. They are limited to four Journal pages. After publication, their full-text papers can also be submitted to this or other journals.
- **Articles** are original full-text reports on innovative, systematic and completed research on catalysis.
- **Highlight Comments** describe and comment on very important new results in the original research of a third person with a view to highlight their significance. The results should be presented clearly but concisely without the comprehensive details required of an original article. Highlight comment should not be more than 2-3 Journal pages (approximately 9000 characters) in length, and should be appropriately organized by the author. Chemical formulae, figures, and schemes should be restricted to important examples. The number of references should be restricted to about 15.
- **Academic Arguments** can discuss, express a different opinion or query the idea, concept, data, data processing method, characterization method, computational method, or the conclusion of published articles. The objective of an academic argument should be to enliven the academic atmosphere.

Impact Factor

2012 SCI Impact Factor: **1.304**
2012 SCI 5-Year Impact Factor: 1.011
2012 ISTIC Impact Factor: 1.198

Abstracting and Indexing

Abstract Journals (VINITI)
Cambridge Scientific Abstracts (CIG)
Catalysts & Catalysed Reactions (RSC)
Current Contents/Engineering, Computing and Technology (Thomson ISI)
Chemical Abstract Service/SciFinder (CAS)
Chemistry Citation Index (Thomson ISI)
Japan Information Center of Science and Technology
Journal Citation Reports/Science Edition (Thomson ISI)
Science Citation Index Expanded (Thomson ISI)
SCOPUS (Elsevier)
Web of Science (Thomson ISI)



中国科学院出版基金资助出版

催化学报

(CUIHUA XUEBAO)

CHINESE JOURNAL OF CATALYSIS

月刊 SCI 收录 2014 年 1 月 第 35 卷 第 1 期



目次

综 述

1 (英)

湿式氧化用于染料废水脱色: 过去 20 年回顾

Jie Fu, George Z. Kyzas

研究论文

8 (英/中/封面文章)

Ni/CeO₂-SiO₂ 催化剂的制备、表征及其甲烷部分氧化制合成气性能

胡久彪, 余长林, 毕亚东, 魏龙福, 陈建钊, 陈喜蓉

21 (英)

聚乙烯基胺包裹 Fe₃O₄@SiO₂ 磁性微球用于 Knoevenagel 缩合

Farzad Zamani, Elham Izadi

28 (英/中)

C₂H₄ 在 Fe₃C(100) 表面吸附及脱氢裂解的密度泛函理论研究

王丙寅, 于小虎, 霍春芳, 王建国, 李永旺

38 (英)

固-溶法制备中温固体氧化物燃料电池高性能

La_{0.8}Sr_{0.2}MnO₃-Ba_{0.5}Sr_{0.5}Co_{0.8}Fe_{0.2}O₃ 阴极

孟丽, 王方中, 王傲, 蒲健, 池波, 李箭

43 (英)

聚(4-乙炔基吡啶)硫酸氢盐: 一个新的高效催化剂用于无溶剂条件下合成 13-芳香基-茚并 [1,2-*b*] 石脑油 [1,2-*e*] 吡喃-12(13*H*)-酮

Majid Ghashang, Syed Sheik Mansoor, Krishnamoorthy Aswin

49 (英)

炭黑颗粒及氟粒子辅助法合成多级结构 MCM-22 分子筛及其催化性能

杨建华, 初筠, 王金渠, 殷德宏, 鲁金明, 张艳

58 (英)

H₃PW₁₂O₄₀ 催化水相介质中苯并恶嗪和喹唑啉合成

Mahmood Tajbakhsh, Rahman Hosseinzadeh, Parizad Rezaee,

Mahgol Tajbakhsh

66 (英/中)

多壁碳纳米管负载 TiO₂ 的光催化脱硝性能

刘浩, 张海茹, 杨宏旻

78 (英)

Ag/Ag₃PO₄/g-C₃N₄ 三元复合光催化剂的制备及其可见光驱动下的光催化活性增强

沈凯, Mohammed Ashraf Gondal, Rashid Ghulam Siddique,

施珊, 王斯琦, 孙江波, 徐庆宇

85 (英)

原位生成的 Ph₃C⁺ 均相有机催化剂催化 4,4'-芳亚甲基-二(3-甲基-1-苯基-1*H*-吡唑-5-醇)高效合成

Abdolkarim Zare, Maria Merajoddin,

Ahmad Reza Moosavi-Zare, Mahmoud Zarei

90 (英/中)

载钛羟基磷灰石光催化降解内分泌干扰物双酚 A

李前, 冯想, 张晓, 宋寒, 张建伟, 尚静, 孙卫玲, 朱彤, 若村正人, 塚田峰春, 陆应亮

99 (英/中)

V₂O₅/赤铁矿催化剂结构及其 NH₃ 选择性催化还原 NO_x 性能

张萍, 陈天虎, 邹雪华, 朱承驻, 陈冬, 刘海波

108 (英/中)

Ag/SBA-15 低温气相选择性催化氧化苯甲醇合成苯甲醛

马良, 贾丽华, 郭祥峰, 项礼军

120 (英)

TiO₂ 晶相对 MnO_x/TiO₂ 催化剂催化 NO 氧化性能的影响

安忠义, 褚玉群, 徐超, 陈昌和

127 (英)

二氧化硫脲: 一锅合成吡喃并 [4,3-*b*] 吡喃类化合物的高效可重复使用有机催化剂

Majid Ghashang, Syed Sheik Mansoor, Krishnamoorthy Aswin

134 (英)

CuCl₂ 和 HY 分子筛的表面反应及 Cu/Y 分子筛的制备及其催化甲醇氧化羰基化

王瑞玉, 李忠

140 (英/中)

MoO₃ 改性的 TiO₂ 在可见光下催化降解亚甲基蓝

杨华博, 李翔, 王安杰, 王瑶, 陈永英

相关信息

148 作者索引

149 《催化学报》作者指南

153 Guide for Authors

英文全文电子版(国际版)由 Elsevier 出版社在 ScienceDirect 上出版

<http://www.sciencedirect.com/science/journal/18722067>

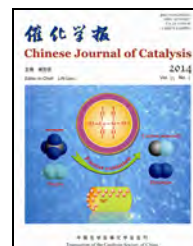
<http://www.elsevier.com/locate/chnjc>

<http://www.chxb.cn>



available at www.sciencedirect.com

journal homepage: www.elsevier.com/locate/chnjc



Chinese Journal of Catalysis Graphical Contents

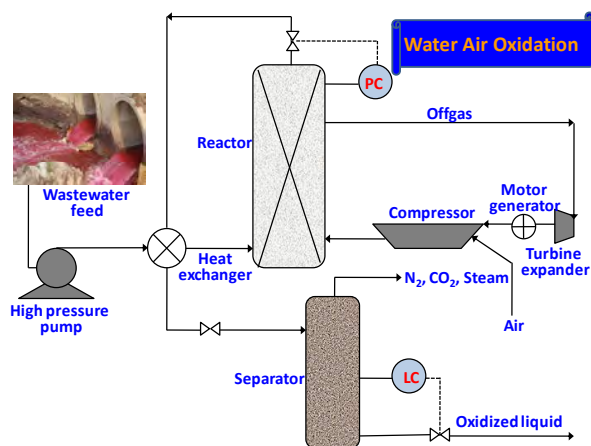
Review

Chin. J. Catal., 2014, 35: 1–7 doi: 10.1016/S1872-2067(12)60724-4

Wet air oxidation for the decolorization of dye wastewater: An overview of the last two decades

Jie Fu, George Z. Kyzas*

Auburn University, USA; Technological Educational Institute of Kavala, Greece; Aristotle University of Thessaloniki, Greece



Wet air oxidation (WAO) is one of the most economically and technologically viable advanced oxidation processes for dye wastewater. The wide studies on WAO of dye wastewater began from 1995. Recent studies focused on real wastewaters.

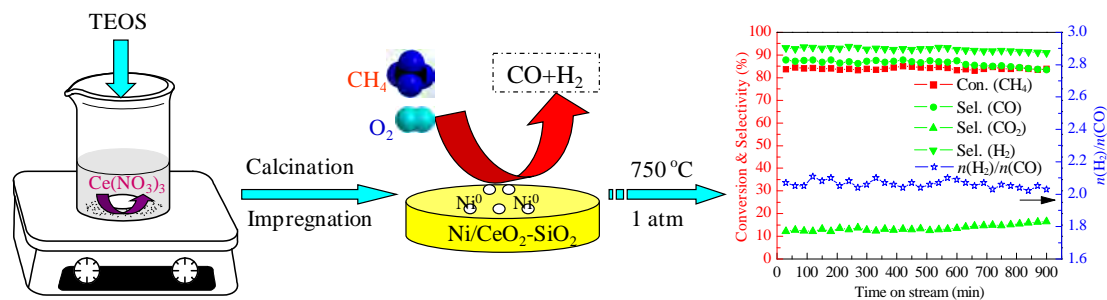
Articles

Chin. J. Catal., 2014, 35: 8–20 doi: 10.1016/S1872-2067(12)60723-2

Preparation and characterization of Ni/CeO₂-SiO₂ catalysts and their performance in catalytic partial oxidation of methane to syngas

Jiubiao Hu, Changlin Yu*, Yadong Bi*, Longfu Wei, Jianchai Chen, Xirong Chen

Jiangxi University of Science and Technology; Tianjin University of Technology



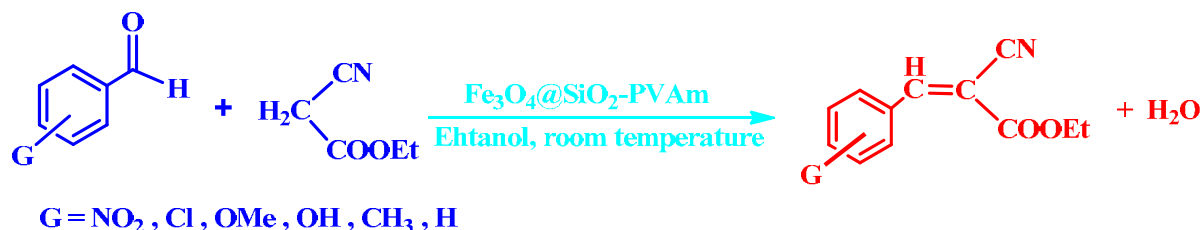
A catalyst consisting of Ni (10%) loaded on a CeO₂-SiO₂ composite support synthesized using a sol-gel process exhibited high performance in the catalytic partial oxidation of methane to syngas, as a result of its large BET surface area, weak acidity, high dispersion, easy of Ni reduction, and low carbon deposition.

Chin. J. Catal., 2014, 35: 21–27 doi: 10.1016/S1872-2067(12)60685-8

Polyvinyl amine coated $\text{Fe}_3\text{O}_4@/\text{SiO}_2$ magnetic microspheres for Knoevenagel condensation

Farzad Zamani*, Elham Izadi

Islamic Azad University, Iran; Isfahan University of Technology, Iran



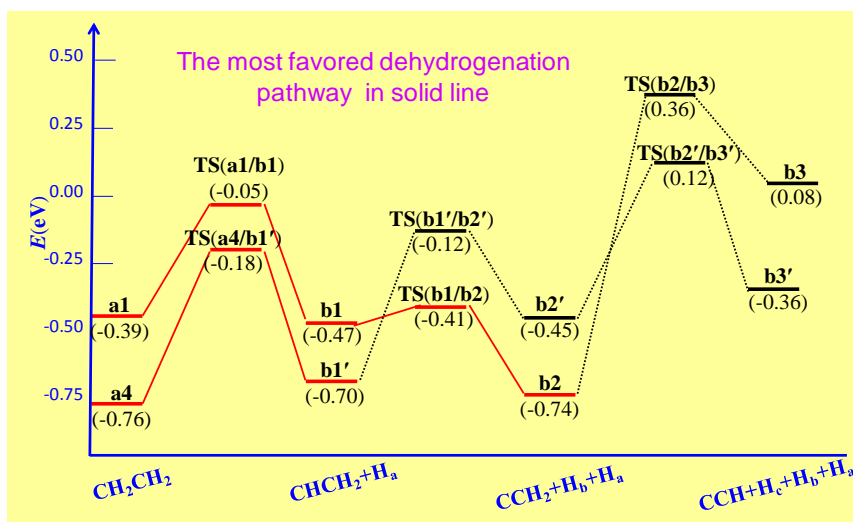
Polyvinyl amine coated $\text{Fe}_3\text{O}_4@/\text{SiO}_2$ was prepared by a simple method. This new magnetic catalyst exhibited high catalytic activity in Knoevenagel condensation of various aromatic and aliphatic aldehydes under mild conditions along with excellent level of reusability.

Chin. J. Catal., 2014, 35: 28–37 doi: 10.1016/S1872-2067(12)60703-7

Density functional theory study of the adsorption and reaction of C_2H_4 on $\text{Fe}_3\text{C}(100)$

Bingyin Wang, Xiaohu Yu, Chunfan Huo*, Jianguo Wang, Yongwang Li

Institute of Coal Chemistry, Chinese Academy of Sciences; University of Chinese Academy of Sciences; Synfuels China Co. Ltd



DFT calculations indicate that on $\text{Fe}_3\text{C}(100)$, C_2H_4 favors dehydrogenation reaction, while the C–C cleavage is not competitive. Vinylidene (CCH_2) and vinyl (CHCH_2) are the most abundant.

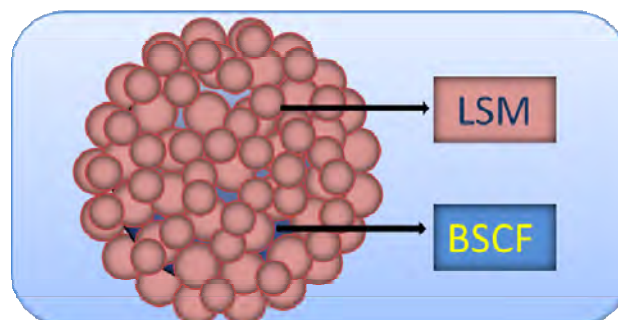
Chin. J. Catal., 2014, 35: 38–42 doi: 10.1016/S1872-2067(12)60704-9

High performance $\text{La}_{0.8}\text{Sr}_{0.2}\text{MnO}_3$ -coated $\text{Ba}_{0.5}\text{Sr}_{0.5}\text{Co}_{0.8}\text{Fe}_{0.2}\text{O}_3$ cathode prepared by a novel solid-solution method for intermediate temperature solid oxide fuel cells

Li Meng, Fangzhong Wang, Ao Wang, Jian Pu, Bo Chi, Jian Li*

Huazhong University of Science and Technology

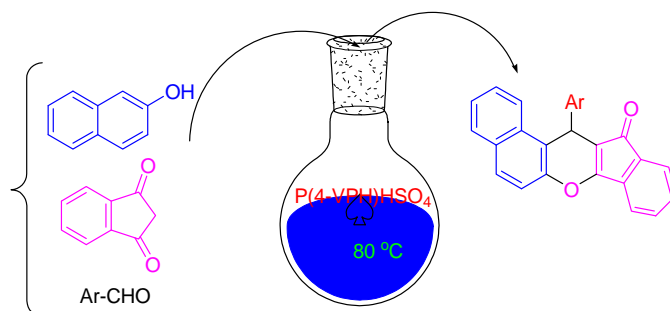
$\text{La}_{0.8}\text{Sr}_{0.2}\text{MnO}_3$ (LSM)-coated $\text{Ba}_{0.5}\text{Sr}_{0.5}\text{Co}_{0.8}\text{Fe}_{0.2}\text{O}_3$ (BSCF) composite powder (LSM-BSCF) synthesized by a novel solid-solution method, exhibited an extended triple phase boundary, reduced LSM polarization resistance, and stabilized microstructure as of the cathode.



Chin. J. Catal., 2014, 35: 43–48 doi: 10.1016/S1872-2067(12)60707-4

Poly(4-vinylpyridinium)hydrogen sulfate: A novel and efficient catalyst for the synthesis of 13-aryl-indeno[1,2-*b*]naphtha[1,2-*e*]pyran-12(13*H*)-ones under solvent-free conditions

Majid Ghashang, Syed Sheik Mansoor*, Krishnamoorthy Aswin
Najafabad Branch, Islamic Azad University, Iran; C. Abdul Hakeem College, India



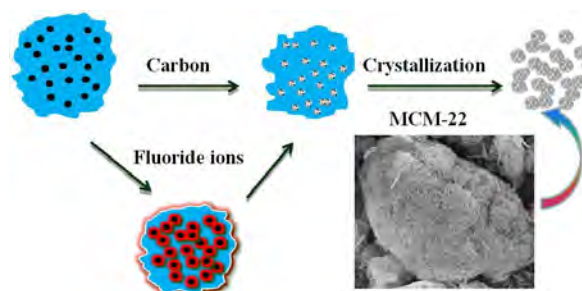
A simple and efficient method for the synthesis of 13-aryl-indeno[1,2-*b*] naphtha[1,2-*e*]pyran-12(13*H*)-ones has been developed that proceeds via a one-pot three-component sequential reaction involving an aromatic aldehyde, β -naphthol, and 2*H*-indene-1,3-dione under solvent-free conditions catalyzed by poly(4-vinylpyridinium)hydrogen sulfate (P(4-VPH)HSO₄).

Chin. J. Catal., 2014, 35: 49–57 doi: 10.1016/S1872-2067(12)60711-6

Synthesis and catalytic performance of hierarchical MCM-22 zeolite aggregates with the assistance of carbon particles and fluoride ions

Jianhua Yang*, Jun Chu, Jinqiu Wang, Dehong Yin, Jinming Lu, Yan Zhang
Dalian University of Technology

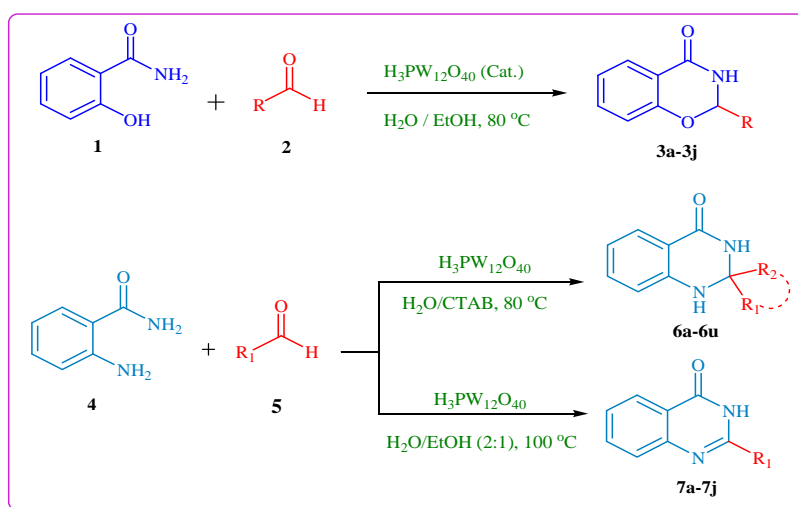
Hierarchical MCM-22 zeolite aggregates constructed by intergrown and stacked thin MCM-22 lamellas were prepared by one-pot hydrothermal synthesis with the assistance of carbon particles and fluoride ions. The Mo/MCM-22-FC catalyst exhibited an improved benzene yield and aromatic selectivity as well as catalyst life in the methane dehydroaromatization reaction.



Chin. J. Catal., 2014, 35: 58–65 doi: 10.1016/S1872-2067(12)60706-2

H₃PW₁₂O₄₀ catalyzed synthesis of benzoxazine and quinazoline in aqueous media

Mahmood Tajbakhsh*, Rahman Hosseinzadeh, Parizad Rezaee, Mahgol Tajbakhsh
University of Mazandaran, Iran



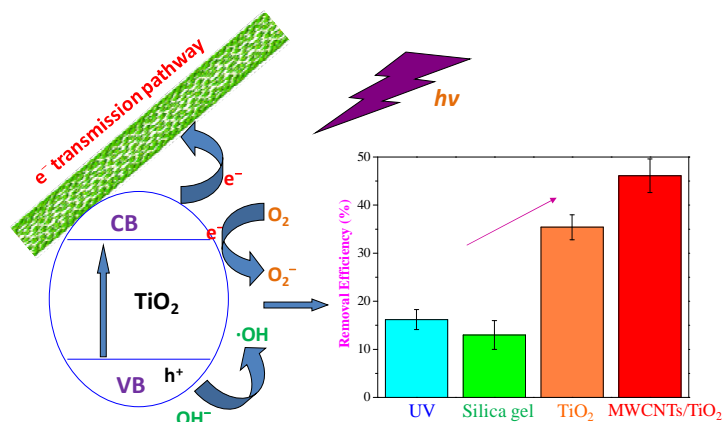
H₃PW₁₂O₄₀ was used as an efficient catalyst for the preparation of benzoxazine and quinazoline ring systems in aqueous media. Advantages include high yields, short reaction times, easy work-up, and green procedure.

Chin. J. Catal., 2014, 35: 66–77 doi: 10.1016/S1872-2067(12)60705-0

Photocatalytic removal of nitric oxide by multi-walled carbon nanotubes-supported TiO₂

Hao Liu, Hairu Zhang, Hongmin Yang*

Nanjing Normal University; Design Institute of Nanjing Shengnuo Heat Pipe Co., Ltd



MWCNTs provide another transfer pathway for photogenerated electrons, assisting in electron and hole separation. This electron-scavenging character of MWCNTs causes MWCNTs/TiO₂ to perform better in photocatalytic denitration than bare TiO₂.

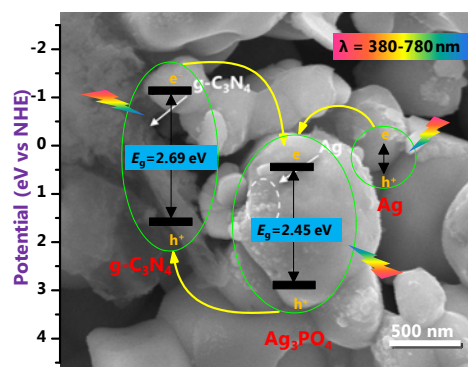
Chin. J. Catal., 2014, 35: 78–84 doi: 10.1016/S1872-2067(12)60712-8

Preparation of ternary Ag/Ag₃PO₄/g-C₃N₄ hybrid photocatalysts and their enhanced photocatalytic activity driven by visible light

Kai Shen*, Mohammed Ashraf Gondal*, Rashid Ghulam Siddique, Shan Shi, Siqi Wang, Jiangbo Sun, Qingyu Xu

Nanjing University of Aeronautics and Astronautics, China;
King Fahd University of Petroleum and Minerals, Saudi Arabia;
Southeast University, China

Ternary Ag/Ag₃PO₄/g-C₃N₄ photocatalyst exhibits excellent photocatalytic activity driven by visible light, attributed to surface plasmon resonance of 40 nm-silver nanoparticles formed on the surface of Ag₃PO₄, and the heterojunction at the interface between Ag₃PO₄ and g-C₃N₄.

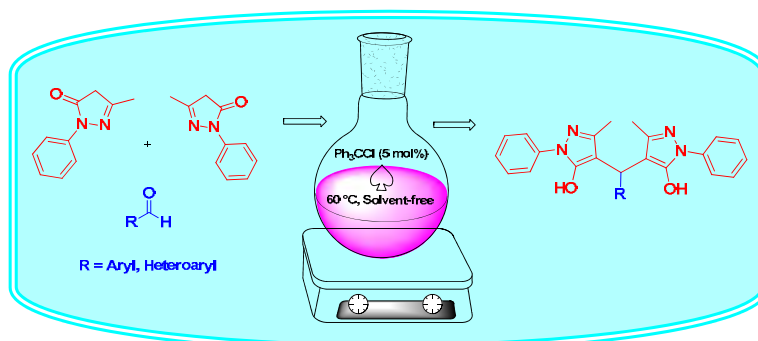


Chin. J. Catal., 2014, 35: 85–89 doi: 10.1016/S1872-2067(12)60728-1

In situ generation of trityl carbocation (Ph₃C⁺) as a homogeneous organocatalyst for the efficient synthesis of 4,4'-(arylmethylene)-bis(3-methyl-1-phenyl-1H-pyrazol-5-ol)s

Abdolkarim Zare*, Maria Merajoddin, Ahmad Reza Moosavi-Zare, Mahmoud Zarei

Payame Noor University, Iran; University of Sayed Jamaledin Asadabadi, Iran; Bu-Ali Sina University, Iran



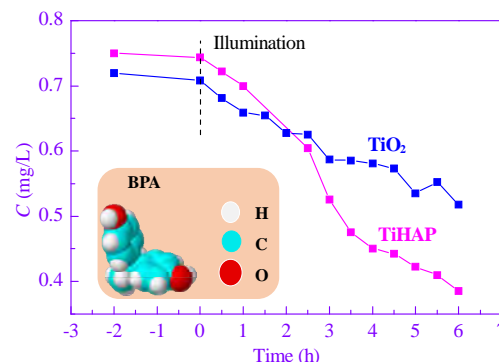
Efficient synthesis of 4,4'-(arylmethylene)-bis(3-methyl-1-phenyl-1H-pyrazol-5-ol)s from 3-methyl-1-phenyl-1H-pyrazol-5(4H)-one and arylaldehydes using Ph₃CCl under solvent-free conditions is described. A plausible reaction mechanism for the process based on the experimental data and that from similar literature studies is proposed.

Chin. J. Catal., 2014, 35: 90–98 doi: 10.1016/S1872-2067(12)60709-8

Photocatalytic degradation of bisphenol A using Ti-substituted hydroxyapatite

Qian Li, Xiang Feng, Xiao Zhang, Han Song, Jianwei Zhang, Jing Shang*, Weiling Sun, Tong Zhu, Masato Wakamura, Mineharu Tsukada, Yingliang Lu
Peking University, China;
Fujitsu Laboratories Limited, Japan;
Fujitsu Research and Development Center, China

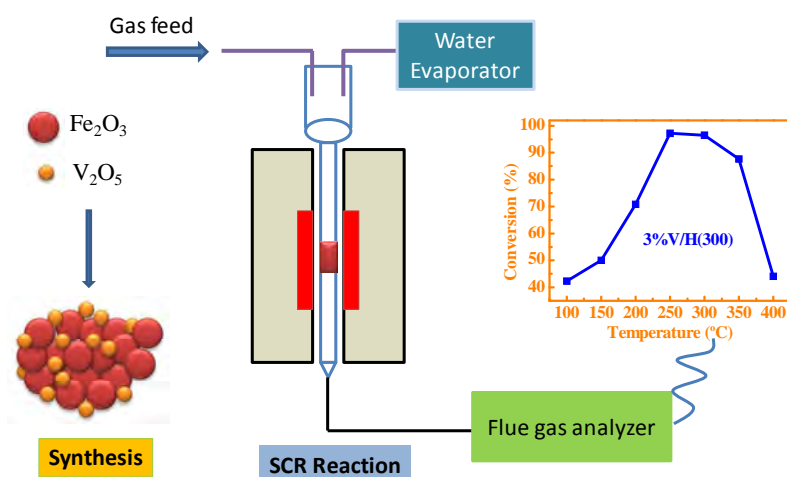
TiHAP film showed an enhanced photocatalytic activity than P25 TiO₂ film for degradation of bisphenol A (BPA), an important kind of environmental endocrine disrupting chemicals.



Chin. J. Catal., 2014, 35: 99–107 doi: 10.1016/S1872-2067(12)60719-0

V₂O₅/hematite catalysts for low temperature selective catalytic reduction of NO_x with NH₃

Ping Zhang, Tianhu Chen*, Xuehua Zou, Chengzhu Zhu, Dong Chen, Haibo Liu
Hefei University of Technology

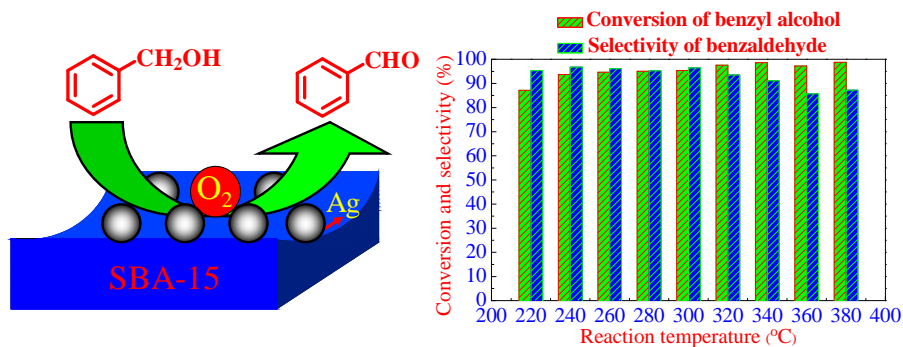


A series of highly dispersed V₂O₅/hematite (V/H) catalysts were prepared by the impregnation of V₂O₅ on goethite, which were highly efficient for the selective catalytic reduction of NO with NH₃.

Chin. J. Catal., 2014, 35: 108–119 doi: 10.1016/S1872-2067(12)60720-7

Catalytic activity of Ag/SBA-15 for low-temperature gas-phase selective oxidation of benzyl alcohol to benzaldehyde

Liang Ma, lihua Jia*, Xiangfeng Guo*, Lijun Xiang
Qiqihar University



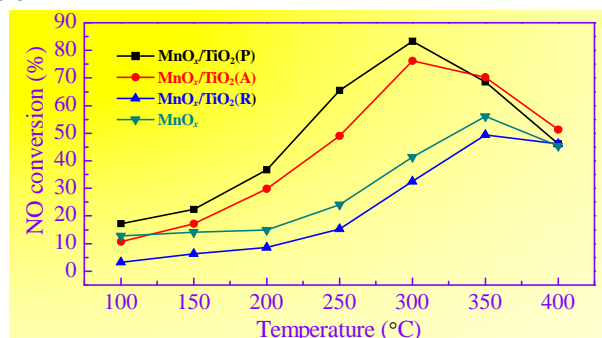
Ag/SBA-15 catalyst for the gas-phase selective oxidation of benzyl alcohol to benzaldehyde with O₂ was prepared using an impregnation method. Ag/SBA-15 displayed good catalytic activity at low temperature and excellent thermal gradient stability.

Chin. J. Catal., 2014, 35: 120–126 doi: 10.1016/S1872-2067(12)60726-8

Influence of the TiO₂ crystalline phase of MnO_x/TiO₂ catalysts for NO oxidation

Zhongyi An, Yuqun Zhuo*, Chao Xu, Changhe Chen
Tsinghua University

Mn-based catalyst supported on P25 TiO₂ was more active for NO oxidation than those supported on anatase and rutile TiO₂, achieving 83% of NO conversion at 300 °C and 20000 h⁻¹ of GHSV.

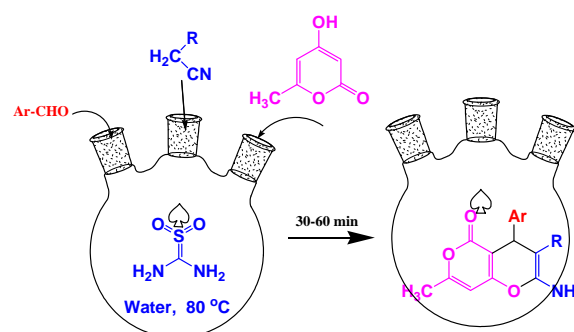


Chin. J. Catal., 2014, 35: 127–133 doi: 10.1016/S1872-2067(12)60727-X

Thiourea dioxide: An efficient and reusable organocatalyst for the rapid one-pot synthesis of pyrano[4,3-*b*]pyran derivatives in water

Majid Ghashang, Syed Sheik Mansoor*, Krishnamoorthy Aswin
Islamic Azad University, Iran;
C. Abdul Hakeem College, India

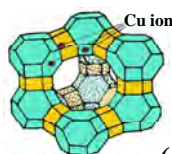
A series of pyrano[4,3-*b*]pyran derivatives have been synthesized by the reaction of aromatic aldehydes with malononitrile or cyanoacetate and 4-hydroxy-6-methylpyran-2-one in water at 80 °C using an aqueous solution of thiourea dioxide as a catalyst in excellent yields.



Chin. J. Catal., 2014, 35: 134–139 doi: 10.1016/S1872-2067(12)60735-9

Surface reaction of CuCl₂ and HY zeolite during the preparation of CuY catalyst for the oxidative carbonylation of methanol

Ruiyu Wang, Zhong Li*
China University of Mining and Technology; Taiyuan University of Technology



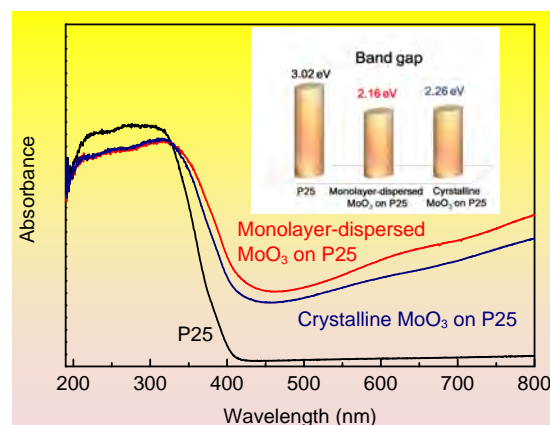
A Cu/Y(CuCl₂) catalyst was prepared by heating a combination of CuCl₂ and HY zeolite, and exhibited higher catalytic activity for the oxidative carbonylation of methanol compared with a conventional Cu/Y catalyst generated by heating a mixture of CuCl and HY zeolite, even though it had lower Cu and Cl contents. In this catalyst, both CuCl and CuCl₂ were present on the surface and ion-exchanged Cu^I and low levels of adsorbed CuCl were in the internal Y zeolite cage structure.

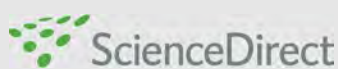
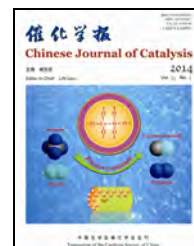
Chin. J. Catal., 2014, 35: 140–147 doi: 10.1016/S1872-2067(12)60731-1

Photocatalytic degradation of methylene blue by MoO₃ modified TiO₂ under visible light

Huabo Yang, Xiang Li*, Anjie Wang, Yao Wang, Yongying Chen
Dalian University of Technology

Strong interactions between the monolayer-dispersed tetrahedral-coordinated molybdenum oxide species and P25 lead to a decrease in the band gap of P25, and thus an increase in its visible light absorption.



available at www.sciencedirect.comjournal homepage: www.elsevier.com/locate/chnjc

Article

Preparation of ternary Ag/Ag₃PO₄/g-C₃N₄ hybrid photocatalysts and their enhanced photocatalytic activity driven by visible light

Kai Shen ^{a,*}, Mohammed Ashraf Gondal ^{b,#}, Rashid Ghulam Siddique ^b, Shan Shi ^a, Siqi Wang ^a, Jiangbo Sun ^a, Qingyu Xu ^c

^a College of Materials Science and Technology, Nanjing University of Aeronautics and Astronautics, Nanjing 211100, Jiangsu, China

^b Laser Research Group, Physics Department and Center of Excellence in Nanotechnology, King Fahd University of Petroleum and Minerals, Dhahran 31261, Saudi Arabia

^c Department of Physics, Southeast University, Nanjing 211189, Jiangsu, China

ARTICLE INFO

Article history:

Received 26 July 2013

Accepted 10 September 2013

Published 20 January 2014

Keywords:

Silver nanoparticle

Silver orthophosphate (Ag₃PO₄)Graphitic carbon nitride (g-C₃N₄)

Surface plasmon resonance

Heterojunction structure

ABSTRACT

The preparation of a series of ternary Ag/Ag₃PO₄/g-C₃N₄ hybrid photocatalysts, which display enhanced photocatalytic activity, was reported. The crystal structure, morphology, composition, optical absorption, and efficient separation of charge carriers were studied by X-ray diffraction, scanning electron microscopy, absorption and photoluminescence spectroscopy measurements. Using rhodamine B as a model contaminant, the as-prepared Ag/Ag₃PO₄/g-C₃N₄ hybrid photocatalyst exhibited superior degradation performance under visible light irradiation than Ag₃PO₄ or binary Ag₃PO₄/g-C₃N₄ hybrid photocatalyst systems. The surface plasmon resonance of the 40 nm-silver nanoparticles formed on the surface of Ag₃PO₄ and the heterojunction formed at the interface between Ag₃PO₄ and g-C₃N₄, are considered to be the major physical-chemical origin and to be responsible for the enhanced photocatalytic activity.

© 2014, Dalian Institute of Chemical Physics, Chinese Academy of Sciences.

Published by Elsevier B.V. All rights reserved.

1. Introduction

Heterogeneous photocatalysis is a promising approach to development of technology for environmental remediation, solar energy conversion, and hydrogen production. The pioneering work of Fujishima et al. [1] spurred interest in the development of visible light driven photocatalysis for application in environmental technology. Subsequent achievements [2–5] have contributed to a drive towards the development of efficient photocatalysts with high quantum efficiency in the visible portion of the solar spectrum (380–780 nm) [6].

Silver orthophosphate (Ag₃PO₄) is an active semiconductor

that can take part in photooxidation processes. Ag₃PO₄ also has a quantum efficiency of 90% at wavelengths longer than 420 nm [7] and shows high photocatalytic activity owing to its absorption in the visible portion of the solar spectrum and high charge carrier mobility. This is because of the delocalized charge distribution of the conduction-band minimum, which results in a small electron effective mass, which is beneficial for the surface carrier mobility [8].

Graphitic carbon nitride (g-C₃N₄) is based on the stacked two-dimensional structure analogous of graphite with N replacing non-adjacent carbon atoms. This material has drawn attention for its potential in water splitting application as a

* Corresponding author. Tel/Fax: +86-25-84895871; E-mail: shenkai84@nuaa.edu.cn

Corresponding author. Tel: +966-3-8602351; Fax: +966-3-8604281; E-mail: magondal@kfupm.edu.sa

This work was supported by the National Natural Science Foundation of China (51172044) and the Project R15-CW-11 (MIT11109, MIT11110) by KFUPM (King Fahd University of Petroleum and Minerals).

DOI: 10.1016/S1872-2067(12)60712-8 | <http://www.sciencedirect.com/science/journal/18722067> | Chin. J. Catal., Vol. 35, No. 1, January 2014

metal-free photocatalyst operating under visible light irradiation, as reported by Wang et al. [9]. However, the potential of this material is limited by inherent constraints such as inefficient use of the visible portion of the solar spectrum and a high electron/hole recombination rate. The photocatalytic efficiency of g-C₃N₄ needs further enhancement prior to any practical application. Various g-C₃N₄ based hybrid photocatalysts including g-C₃N₄/BiPO₄ [10], graphene/g-C₃N₄ [11], g-C₃N₄/Bi₂WO₆ [12], Fe-g-C₃N₄-LUS-1 [13], g-C₃N₄/SiO₂-HNb₃O₈ [14], and g-C₃N₄/TaON [15] have been developed to further extend the visible light absorption range and the photogenerated carriers separation efficiency.

Described herein is a simple photochemical precipitation based preparation of a series of novel ternary Ag/Ag₃PO₄/g-C₃N₄ hybrid photocatalysts and a detailed investigation of the catalytic activity using rhodamine B (RhB) as a model contaminant. Our photocatalytic experiments indicate that the Ag/Ag₃PO₄/g-C₃N₄ hybrid system exhibits superior photocatalytic performance for RhB degradation compared with a binary Ag₃PO₄/g-C₃N₄ photocatalyst, or Ag₃PO₄ and g-C₃N₄ as individual components. It was found that RhB photodegradation strongly depends on the proportion of silver nanoparticles on the Ag₃PO₄ surface and the ratio of the components in the Ag₃PO₄/g-C₃N₄ hybrid. The enhanced photoactivity can be attributed to the surface plasmon resonance (SPR) originating from silver nanoparticles and the heterojunction-like interface between Ag₃PO₄ and g-C₃N₄. This work is a continuation of our commitment to developing environmentally friendly technologies for clean fuel by using the photocatalytic technique [16–21].

2. Experimental

2.1. Materials

All the chemicals used in this study were of analytical grade and used as received without further purification. Absolute ethanol (C₂H₅OH), sodium bismuthate (NaBiO₃), disodium hydrogen phosphate (Na₂HPO₄), anatase-TiO₂, and rhodamine B (RhB) were purchased from Sinopharm Chemical Reagent Co. Melamine and silver nitrate (AgNO₃) were obtained from Shanghai Lingfeng Chemical Reagent Co. Ltd and Jiangsu Qiangsheng Chemical Co. Ltd, respectively. Distilled water was produced using a Direct-Q Millipore filtration system to a resistivity of 18.2 MΩcm (Millipore Limited, Watford, UK).

2.2. Preparation

g-C₃N₄ was prepared through a pyrolysis process using melamine as the starting material [22], and then binary Ag₃PO₄/g-C₃N₄ (*x*) (where *x* denotes the mass fraction of Ag₃PO₄ in the sample) hybrid photocatalysts were prepared by a chemical deposition-precipitation method. In a typical preparation for the case of Ag₃PO₄/g-C₃N₄ (0.8), 2.3 g of g-C₃N₄ was dispersed into an aqueous solution of AgNO₃ (1.26 g/50 mL). Then a solution of Na₂HPO₄ (0.9 g/50 mL) was added drop-wise over 30 min into the above suspension with stirring

until the precipitation was completed. The mixture was then centrifuged, washed with water, and dried overnight at 50 °C. The obtained Ag₃PO₄/g-C₃N₄ (0.8) powder (2.0 g) was dispersed in 200 mL of water and irradiated by a 300 W Xenon lamp (Beijing Trusttech Co. Ltd., PLS-SXE-300) equipped with a visible light band pass filter (400–800 nm) for 0.5–3 h. The final product was collected by centrifugation at 4000 r/min, washed with absolute ethanol/water several times, and then dried at 50 °C. The series of Ag/Ag₃PO₄/g-C₃N₄ hybrid photocatalysts were denoted Ag/Ag₃PO₄/g-C₃N₄ (*x*; *t*), where *t* is the irradiation time (0.5–3 h) for the preparation.

2.3. Characterization

The crystal structure of the ternary Ag/Ag₃PO₄/g-C₃N₄ hybrid photocatalysts was analyzed using a wide-angle X-ray diffractometer (Rigaku SmartLab) employing Cu K_α radiation ($\lambda = 0.15418$ nm). Scanning electron microscope (SEM) imaging of samples was performed using a FEI F50 SEM. Diffuse reflectance of samples was measured with a JASCO V-670 UV-Vis-NIR spectrophotometer. The photoluminescence (PL) spectra were recorded on a PL spectrofluorometer (Horiba Jobin) at an excitation wavelength of 365 nm.

2.4. Photocatalytic evaluation

The degradation of RhB was used as a model reaction to evaluate photodegradation behavior of the ternary Ag/Ag₃PO₄/g-C₃N₄ hybrid photocatalyst. For the photodegradation experiments, a 150 mL solution of RhB (7 mg/L) was prepared, into which 150 mg of photocatalyst was added. The suspension of the RhB solution and photocatalyst was magnetically stirred in the dark for 60 min to ensure adsorption-desorption equilibrium before the irradiation. The suspension was then irradiated with a 300 W Xenon lamp equipped with visible light band pass filter (400–800 nm). Portions of the reaction mixture slurry were taken from the mixture and filtered to remove Ag/Ag₃PO₄/g-C₃N₄ hybrid photocatalyst at regular intervals. The concentration of RhB in the aqueous solution was determined using a UV-VIS spectrophotometer (Hitachi U-3900).

3. Results and discussion

3.1. Structure and composition of synthesized catalysts

Figure 1 depicts XRD patterns of the ternary Ag/Ag₃PO₄/g-C₃N₄ hybrid photocatalyst prepared at different exposure time. The diffraction peaks of both g-C₃N₄ and silver nanoparticles cannot be observed clearly in XRD patterns because of strong interference with the Ag₃PO₄ signals. However, a new peak appeared at 38.1° in the Ag₃PO₄/g-C₃N₄ sample irradiated for 3 h that could be indexed as the silver (111).

The enlarged XRD patterns (Fig. 2) from 37° to 40° and 26.5° to 29° show the Ag(111) and g-C₃N₄(002) peaks, respectively. These results confirmed the formation of silver particles on the surface of the Ag₃PO₄ particles and the existence of a g-C₃N₄ phase. The diffraction intensity of the Ag(111) peak

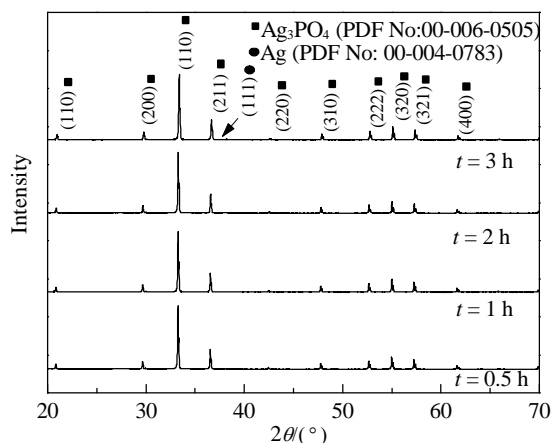


Fig. 1. XRD patterns of series ternary Ag/Ag₃PO₄/g-C₃N₄ hybrid photocatalysts prepared under visible light exposure for 0.5, 1, 2, and 3 h.

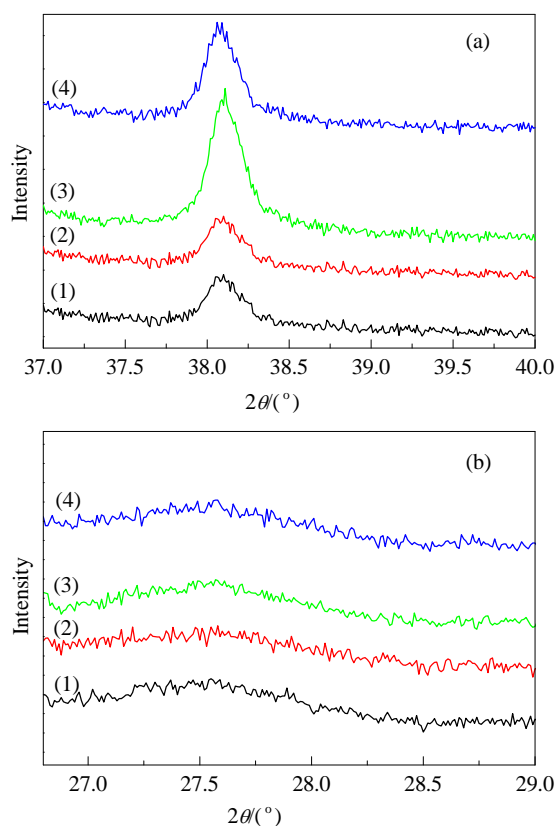


Fig. 2. Enlarged XRD patterns of Ag(111) (a) and g-C₃N₄(002) (b) diffraction peaks from series ternary Ag/Ag₃PO₄/g-C₃N₄ photocatalysts prepared under visible light exposure for 0.5 (1), 1 (2), 2 (3), and 3 h (4).

increased and saturated with prolonged irradiation time, which may suggest that the silver nanoparticles formed in situ on surface of Ag₃PO₄ and inhibited further photochemical reduction of the Ag₃PO₄ to Ag⁰. The size of the silver nanoparticles from different light exposed samples was calculated and summarized in Table 1 using the Scherrer equation based on full width at half maximum (FWHM) value for Ag(111) peak at 38.1°. By a semi quantitative analysis, 0.6%, 1.0%, 2.1%, and 2.8% metallic silver was estimated in samples irradiated for

Table 1

Calculated particle sizes and composition ratios of silver nanoparticles.

<i>t</i> /h	FWHM (Ag(111))/(°)	Particle size (nm)	w(Ag)/%
0.5	0.220	39.7	0.6
1	0.241	36.0	1.0
2	0.245	35.5	2.1
3	0.232	37.6	2.8

0.5, 1, 2, and 3 h, respectively. Figure 3 shows a typical SEM image of Ag/Ag₃PO₄/g-C₃N₄ (0.8; 1 h) photocatalyst. The silver nanoparticles can be clearly seen in the SEM images, and the particle size is estimated at around 40–50 nm, which is in agreement with the XRD analysis.

3.2. Optical properties of synthesized photocatalysts

Figure 4 illustrates the optical absorption spectra of g-C₃N₄, Ag₃PO₄, Ag₃PO₄/g-C₃N₄ (0.8), and Ag/Ag₃PO₄/g-C₃N₄ (0.8; 1 h). The peaks at around 393 and 454 nm in the ternary Ag/Ag₃PO₄/g-C₃N₄ hybrid photocatalyst can be attributed to the absorptions of g-C₃N₄ and Ag₃PO₄, respectively. Ag/Ag₃PO₄/g-C₃N₄ exhibits much higher absorption, which may be attributed to the surface plasmon resonance (SPR) of the silver nanoparticles [23].

PL spectra of g-C₃N₄ and Ag/Ag₃PO₄/g-C₃N₄ (0.8; *t*) samples

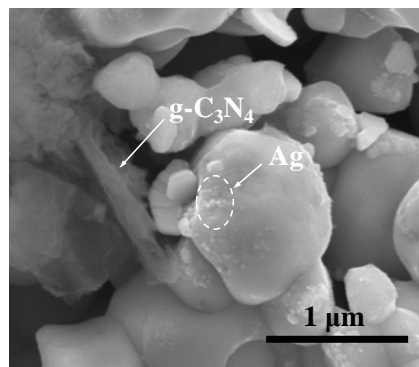


Fig. 3. SEM image of as-prepared ternary Ag/Ag₃PO₄/g-C₃N₄ (0.8; 1 h) hybrid photocatalyst.

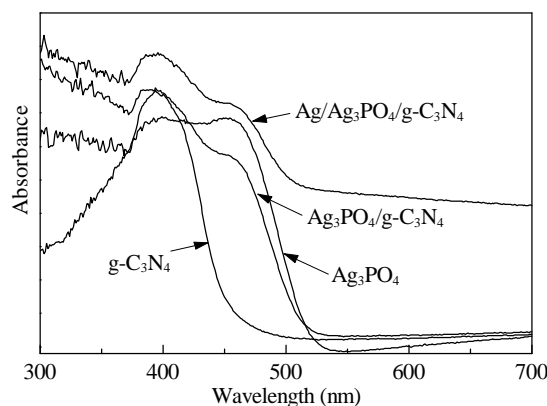


Fig. 4. UV-Vis absorption spectra of ternary Ag/Ag₃PO₄/g-C₃N₄ (0.8; 1 h) hybrid photocatalyst, binary Ag₃PO₄/g-C₃N₄ (0.8) photocatalyst, Ag₃PO₄, and g-C₃N₄.

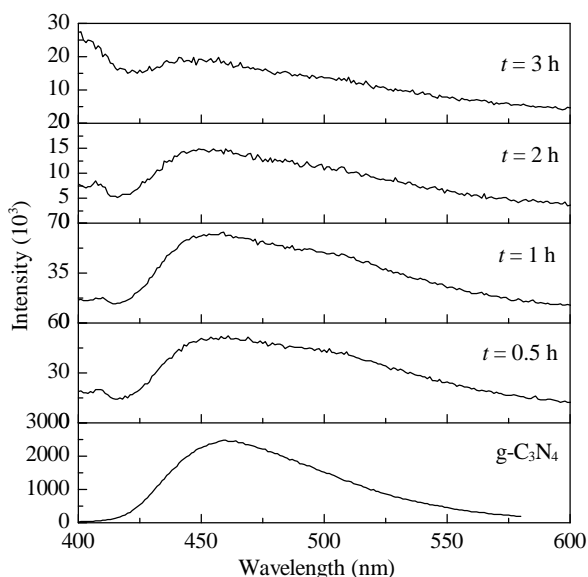


Fig. 5. PL spectra of series ternary Ag/Ag₃PO₄/g-C₃N₄ (0.8; *t*) hybrid photocatalysts and g-C₃N₄ semiconductor.

are shown in Fig. 5. A strong emission band centered at 459 nm in g-C₃N₄ can be assigned to the emission of g-C₃N₄ with an energy corresponding to its band gap. This indicates more efficient radiative recombination of the photogenerated carriers inside the g-C₃N₄ semiconductor in samples prepared with longer irradiation time. The overall PL emission intensity of the Ag/Ag₃PO₄/g-C₃N₄ (0.8; *t*) hybrid photocatalysts decreased with respect to the overall PL intensity of g-C₃N₄ with increasing irradiation time. This may be attributed to charge transfer between Ag₃PO₄ and g-C₃N₄ or trapping of photoexcited electrons by the silver nanoparticles.

3.3. Photocatalytic activity

The effect of the Ag₃PO₄/C₃N₄ mass ratio from Ag₃PO₄ to g-C₃N₄ on the photodegradation performance was investigated before studying the enhancement of photodegradation by the silver nanoparticles in the ternary systems. Figure 6 illustrates the photocatalytic activity of a series of Ag₃PO₄/g-C₃N₄ hybrid photocatalysts investigated. The Ag₃PO₄/g-C₃N₄ hybrid photocatalysts showed considerably enhanced photocatalytic performance compared with either Ag₃PO₄ or g-C₃N₄ alone, suggesting a synergic effect as reported by Zhang et al. [24] and Kumar et al. [25]. The optimum composition ratio was found to be 4:1 for the Ag₃PO₄/g-C₃N₄ hybrid, and this photocatalyst completely decomposed the model contaminant over the course of the experiment. Only 63% and 12% degradation of RhB were observed within 30 min using pure Ag₃PO₄ and g-C₃N₄, respectively.

The curves in Fig. 7 depict the removal of RhB as a function of irradiation time using the ternary Ag/Ag₃PO₄/g-C₃N₄ hybrid photocatalysts. Further enhancement in photodegradation performance was observed from the as-prepared Ag/Ag₃PO₄/g-C₃N₄ samples. Almost 50% of the RhB in the aqueous suspension was decomposed using Ag/Ag₃PO₄/g-C₃N₄ (0.8; 1 h) under

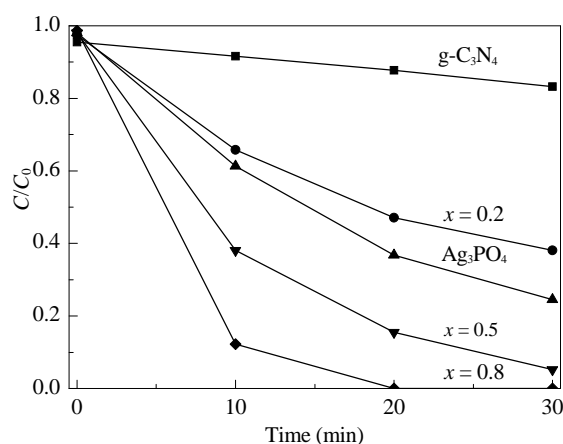


Fig. 6. Changes of RhB concentration over a series of binary Ag₃PO₄/g-C₃N₄ (*x* = 0, 0.2, 0.5, 0.8, 1) photocatalysts.

broadband visible light irradiation for 5 min. This ratio may be considered as the optimal compositional ratio of the ternary photocatalyst. Around 40% degradation was obtained from Ag₃PO₄/g-C₃N₄ (0.8) under identical experimental conditions.

The corresponding UV-Vis spectral changes (inset in Fig. 7) show the intensity of the absorption peak at 554 nm decreasing dramatically as the photodegradation reaction progresses. It is notable that no blue-shift of the RhB absorption peak centered at 554 nm was observed, suggesting a decomposition mecha-

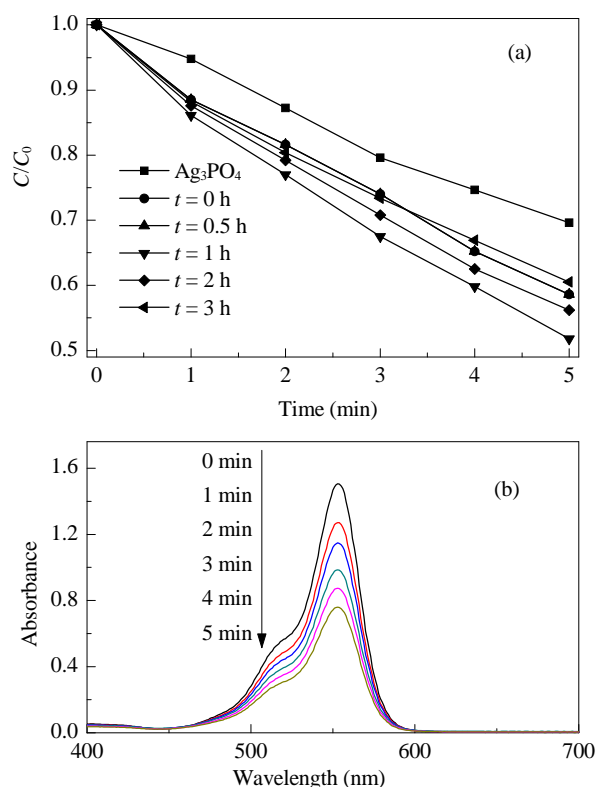


Fig. 7. (a) Changes of the RhB concentration over series ternary Ag/Ag₃PO₄/g-C₃N₄ (0.8; *t*) hybrid photocatalysts; (b) Changes to the UV-Vis spectra of the RhB with Ag/Ag₃PO₄/g-C₃N₄ (0.8; 1 h) as a function of irradiation time.

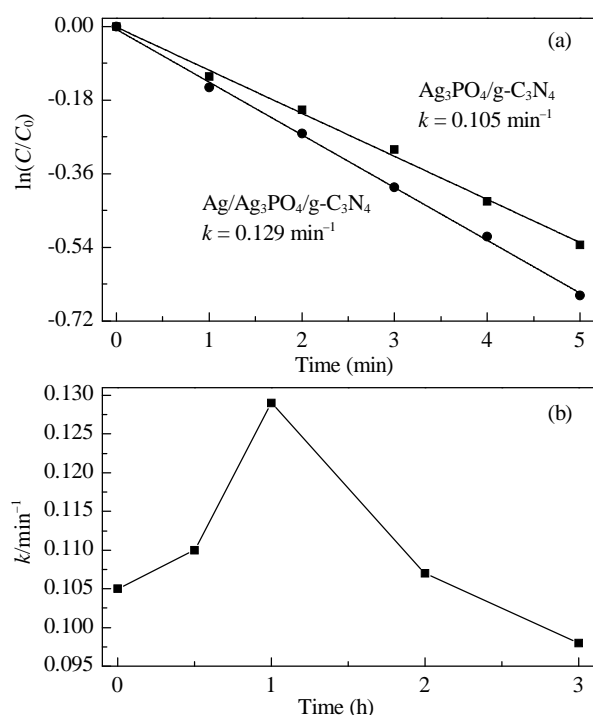


Fig. 8. (a) Comparison of rate constants (fitted by pseudo-1st-order kinetic model) of $\text{Ag}_3\text{PO}_4/\text{g-C}_3\text{N}_4$ (0.8) and as-prepared $\text{Ag}/\text{Ag}_3\text{PO}_4/\text{g-C}_3\text{N}_4$ (0.8; 1 h) hybrid photocatalyst. (b) Changes of rate constants on the irradiation time in the preparation of $\text{Ag}/\text{Ag}_3\text{PO}_4/\text{g-C}_3\text{N}_4$ (0.8; 0–3 h).

nism involving cleavage of the whole conjugated chromophore structure in RhB during the photochemical reaction, rather than an N-deethylation process [26].

Figure 8 shows a comparison of the apparent rate constants (k) of the $\text{Ag}/\text{Ag}_3\text{PO}_4/\text{g-C}_3\text{N}_4$ (0.8; 1 h) hybrid photocatalysts and $\text{Ag}_3\text{PO}_4/\text{g-C}_3\text{N}_4$ calculated by the Langmuir-Hinshelwood model [27]. Using the binary $\text{Ag}_3\text{PO}_4/\text{g-C}_3\text{N}_4$ photocatalyst as a baseline, an apparent rate of 0.105 min^{-1} was obtained for the reaction in the first 5 min. The $\text{Ag}/\text{Ag}_3\text{PO}_4/\text{g-C}_3\text{N}_4$ hybrid photocatalyst prepared by light irradiation for 1 h showed a 25% enhancement (0.129 min^{-1}). Figure 8 (b) shows the effect of irradiation time during the preparation of $\text{Ag}/\text{Ag}_3\text{PO}_4/\text{g-C}_3\text{N}_4$ (i.e. which correlates with the loading of silver nanoparticles) on the kinetic rate constant. It is clear that the kinetic rate constant increases initially with the silver nanoparticle loading and subsequently decreases. The highest performance was obtained from $\text{Ag}/\text{Ag}_3\text{PO}_4/\text{g-C}_3\text{N}_4$ (0.8; 1 h).

Compared with other popular photocatalytic systems, the as-prepared ternary $\text{Ag}/\text{Ag}_3\text{PO}_4/\text{g-C}_3\text{N}_4$ (0.8; 1 h) hybrid photocatalyst exhibits superior performance. A comparison shown in Fig. 9 suggests that the kinetic rate constant of $\text{Ag}/\text{Ag}_3\text{PO}_4/\text{g-C}_3\text{N}_4$ (0.8; 1 h) at 0.129 min^{-1} within 6 min is higher than the kinetic rate constants observed on anatase TiO_2 (0.009 min^{-1}), P25 (0.016 min^{-1}), NaBiO_3 (0.054 min^{-1}), Ag_3PO_4 (0.073 min^{-1}), and $\text{Ag}_3\text{PO}_4/\text{g-C}_3\text{N}_4$ (0.8) (0.105 min^{-1}). The low photodegradation rate of RhB on TiO_2 (or P25) may be attributed to the wide band gap of the materials, which restricts photosensitization by visible light [28]. Compared with the commercial photocatalyst

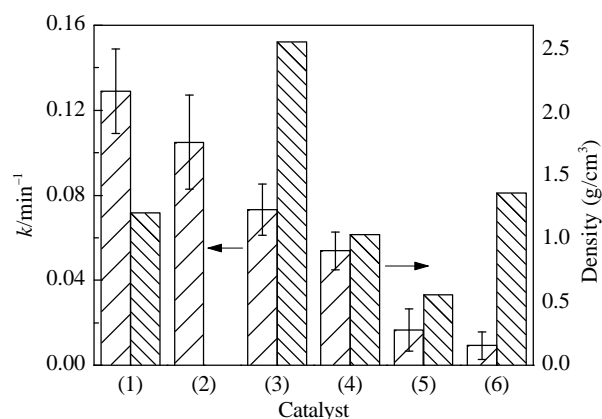


Fig. 9. Comparison of photocatalytic performance and solid density of various photocatalysts. (1) $\text{Ag}/\text{Ag}_3\text{PO}_4/\text{g-C}_3\text{N}_4$; (2) $\text{Ag}_3\text{PO}_4/\text{g-C}_3\text{N}_4$; (3) Ag_3PO_4 ; (4) NaBiO_3 ; (5) P25; (6) Anatase TiO_2 .

P25, a 6-fold improvement of photodegradation activity was achieved for the $\text{Ag}/\text{Ag}_3\text{PO}_4/\text{g-C}_3\text{N}_4$ (0.8; 1 h) hybrid photocatalyst. In addition, as shown in Fig. 9, the high density of the hybrid photocatalyst ($\rho = 1.2 \text{ g/cm}^3$) indicates that it would be more convenient to separate it from the aqueous phase for regeneration and reuse, compared with P25 ($\rho = 0.56 \text{ g/cm}^3$).

The proposed ternary $\text{Ag}/\text{Ag}_3\text{PO}_4/\text{g-C}_3\text{N}_4$ hybrid photocatalyst can be easily recycled using a simple filtration technique and then washed with water to remove adsorbed RhB. As depicted in Fig. 10, after the first three cycles, the kinetic rate constants remained above 0.12 min^{-1} . The kinetic constant rate decreased to 0.04 min^{-1} after the 6th cycle, likely because of catalyst fouling [29].

3.4. Possible mechanisms of decomposition

The adsorption of RhB molecules to the Ag_3PO_4 or $\text{g-C}_3\text{N}_4$ photocatalyst surfaces was investigated, revealing that less than 4% of the RhB adsorbed to Ag_3PO_4 or $\text{g-C}_3\text{N}_4$. The weak interaction of the RhB with this material may be considered one of the reasons for the enhanced photoactivity following introduction of silver nanoparticles. It is also notable that the enhancement in activity arises from the bifunctional heterojunction structure at the interface of $\text{Ag}_3\text{PO}_4/\text{g-C}_3\text{N}_4$, as indi-

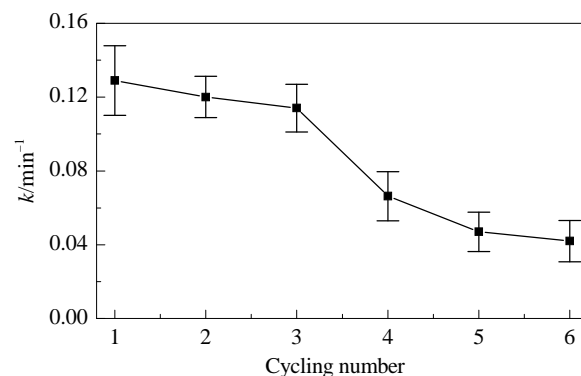


Fig. 10. Changes of the rate constant (fitted by pseudo-1st-order kinetic model) of RhB decomposition on ternary $\text{Ag}/\text{Ag}_3\text{PO}_4/\text{g-C}_3\text{N}_4$ (0.8; 1 h) over six successive photodegradation cycles.

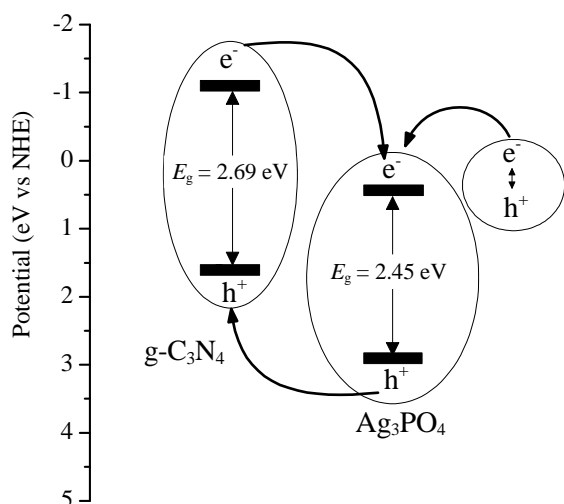


Fig. 11. Possible mechanism of photoactivity enhancement onto ternary Ag/Ag₃PO₄/g-C₃N₄ hybrid photocatalyst by fast separation of carriers.

cated by PL data and the SPR from the silver nanoparticles of the ternary Ag/Ag₃PO₄/g-C₃N₄ hybrid photocatalyst. The proposed mechanism of charge carrier separation in system is illustrated in Fig. 11.

It is reported [24,25] that the conduction band edges of g-C₃N₄ and Ag₃PO₄ are at -1.12 eV and 0.45 eV (vs NHE), respectively. Thus photoexcited electrons from the conduction band (CB) of g-C₃N₄ are injected into the CB of Ag₃PO₄ because of favorable offset between the CB edges of g-C₃N₄ and Ag₃PO₄ as illustrated in Fig. 11. The photogenerated holes move from the valence band (VB) of the Ag₃PO₄ towards the VB of g-C₃N₄ because of the more positive VB edge of Ag₃PO₄ (2.9 eV, vs NHE) than that of g-C₃N₄ (1.57 eV, vs NHE).

Harnessing the plasmonic effects of silver nanoparticles, to generate highly-active composite photocatalysts through combining the nanoparticles with semiconducting materials has been reported including Ag-TiO₂ nanocomposite hollow spheres [30] and Ag/AgCl/TiO₂ nanotube arrays [31], etc. Our previous simulation results [32] have clearly shown that the highest surface plasmon polariton momentum of silver nanoparticles is achieved by irradiation of photons with a wavelength of 359 nm in RhB aqueous solution, by considering the Brendel-Bormann model. The surface plasmon polariton momentum is decreased by 25% when changing the wavelength of the excitation source from 359 to 400 nm. This may also explain why the apparent photocatalytic enhancement of the Ag/Ag₃PO₄/g-C₃N₄ hybrid photocatalyst can be observed under visible light irradiation between 400 and 800 nm, even though the most efficient excitation wavelength for the SPR effect is $\lambda = 359$ nm, which has a naturally low intensity in the solar spectrum. Decreased catalytic activity was observed for samples that were highly decorated with silver nanoparticles. Further reduction of silver on the surface of Ag₃PO₄ not only destroyed the SPR because of agglomeration of silver nanoparticles but also reduced the surface area available for the reaction on Ag₃PO₄.

4. Conclusions

The preparation of a ternary Ag/Ag₃PO₄/g-C₃N₄ hybrid photocatalyst and its improved photodegradation performance are reported. The highest photoactivity was achieved by optimization of the silver nanoparticle ($w = 1.0\%$) surface coverage on the Ag₃PO₄ and the composition fraction ($x = 0.8$) of Ag₃PO₄ and g-C₃N₄. The as prepared hybrid photocatalyst can be regenerated and separated from the aqueous phase easily. In addition, the catalyst also exhibits high photostability under visible light exposure and shows enhanced photodegradation of RhB dye in solution compared with other typical photocatalysts.

References

- [1] Fujishima A, Honda K. *Nature*, 1972, 238: 37
- [2] Asahi R, Morikawa T, Ohwaki T, Aoki K, Taga Y. *Science*, 2001, 293: 269
- [3] Zou Z G, Ye J H, Sayama K, Arakawa H. *Nature*, 2001, 414: 625
- [4] Kudo A, Miseki Y. *Chem Soc Rev*, 2009, 38: 253
- [5] Zhang Y, Pan Z M, Wang X C. *Chin J Catal* (郑云, 潘志明, 王心晨. 催化学报), 2013, 34: 524
- [6] Wang W, Lu C H, Su M X, Ni Y R, Xu Z Z. *Chin J Catal* (王卫, 陆春华, 苏明星, 倪亚茹, 许仲梓. 催化学报), 2012, 33: 629
- [7] Yi Z G, Ye J H, Kikugawa N, Kako T, Ouyang S X, Stuart-Williams H, Yang H, Cao J Y, Luo W J, Li Z S, Liu Y, Withers R. *Nat Mater*, 2010, 9: 559
- [8] Umezawa N, Ouyang S X, Ye J H. *Phys Rev B*, 2011, 83: 035202
- [9] Wang X C, Maeda K, Thomas A, Takanabe K, Xin G, Carlsson J M, Domen K, Antonietti M. *Nat Mater*, 2009, 8: 76
- [10] Pan C S, Xu J, Wang Y J, Li D, Zhu Y F. *Adv Funct Mater*, 2012, 22: 1518
- [11] Xiang Q J, Yu J G, Jaroniec M. *J Phys Chem C*, 2011, 115: 7355
- [12] Ge L, Han C C, Liu J. *Appl Catal B*, 2011, 108-109: 100
- [13] Shiravand G, Badiei A, Ziarani G M, Jafarabadi M, Hamzehloo M. *Chinese J Catal* (催化学报), 2012, 33: 1347
- [14] Pan H Q, Li X K, Zhuang Z J, Zhang C. *J Mol Catal A*, 2011, 345: 90
- [15] Yan S C, Lü S B, Li Z S, Zou Z G. *Dalton Trans*, 2010, 39: 1488
- [16] Gondal M A, Rashid S G, Dastageer M A, Zubair S M, Ali M A, Lienhard J H, McKinley G, Varanasi K K. *IEEE Photonics J*, 2013, 5: 2201908
- [17] Gondal M A, Ali M A, Dastageer M A, Chang X F. *Catal Lett*, 2013, 143: 108
- [18] Shen K, Gondal M A, Li Z J, Li L Y, Xu Q Y, Yamani Z H. *React Kinet Mechan Catal*, 2013, 109: 247
- [19] Zhang J, Gondal M A, Wei W, Zhang T N, Xu Q Y, Shen K. *J Alloys Compd*, 2012, 530: 107
- [20] Luo L R, Shen K, Xu Q Y, Zhou Q, Wei W, Gondal M A. *J Alloys Compd*, 2013, 558: 73
- [21] Zhang B, Ji G B, Gondal M A, Liu Y S, Zhang X M, Chang X F, Li N W. *J Nanopart Res*, 2013, 15: 1773
- [22] Yan S C, Li Z S, Zou Z G. *Langmuir*, 2009, 25: 10397
- [23] Bhui D K, Bar H, Sarkar P, Sahoo G P, De S P, Misra A. *J Mol Liq*, 2009, 145: 33
- [24] Zhang F J, Xie F Z, Zhu S F, Liu J, Zhang J, Mei S F, Zhao W. *Chem Eng J*, 2013, 228: 435
- [25] Kumar S, Surendar T, Baruah A, Shanker V. *J Mater Chem A*, 2013, 1: 5333
- [26] Wang Q, Chen C C, Zhao D, Ma W H, Zhao J C. *Langmuir*, 2008, 24:

Graphical Abstract

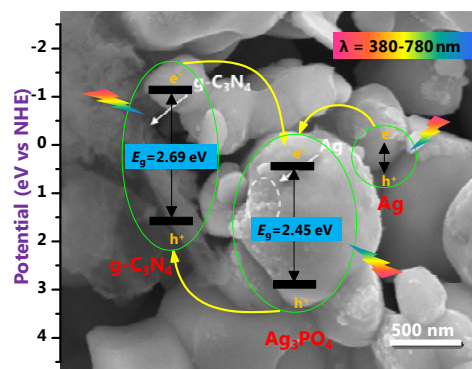
Chin. J. Catal., 2014, 35: 78–84 doi: 10.1016/S1872-2067(12)60712-8

Preparation of ternary Ag/Ag₃PO₄/g-C₃N₄ hybrid photocatalysts and their enhanced photocatalytic activity driven by visible light

Kai Shen*, Mohammed Ashraf Gondal*, Rashid Ghulam Siddique, Shan Shi, Siqi Wang, Jiangbo Sun, Qingyu Xu

Nanjing University of Aeronautics and Astronautics, China;
King Fahd University of Petroleum and Minerals, Saudi Arabia;
Southeast University, China

Ternary Ag/Ag₃PO₄/g-C₃N₄ photocatalyst exhibits excellent photocatalytic activity driven by visible light, attributed to surface plasmon resonance of 40 nm-silver nanoparticles formed on the surface of Ag₃PO₄, and the heterojunction at the interface between Ag₃PO₄ and g-C₃N₄.



7338

[27] Park C Y, Ghosh T, Meng Z D, Kefayat U, Vikram N, Oh W C. *Chin J Catal* (催化学报), 2013, 34: 711

[28] Chen C C, Ma W H, Zhao J C. *Chem Soc Rev*, 2010, 39: 4206

[29] Wang W G, Cheng B, Yu J G, Liu G, Fan W H. *Chem Asian J*, 2012, 7:

1902

[30] Xiang Q J, Yu J G, Cheng B, Ong H C. *Chem Asian J*, 2010, 5: 1466

[31] Yu J G, Dai G P, Huang B B. *J Phys Chem C*, 2009, 113: 16394

[32] Gondal M A, Chang X F, Sha W E I, Yamani Z H, Zhou Q. *J Colloid Interf Sci*, 2013, 392: 325

Ag/Ag₃PO₄/g-C₃N₄三元复合光催化剂的制备及其可见光驱动下的光催化活性增强

沈 凯^{a,*}, Mohammed Ashraf Gondal^{b,#}, Rashid Ghulam Siddique^b,

施 珊^a, 王斯琦^a, 孙江波^a, 徐庆宇^c

^a南京航空航天大学材料科学与技术学院, 江苏南京211100

^b法赫德国王石油与矿业大学物理系, 达兰31261, 沙特阿拉伯

^c东南大学物理系, 江苏南京211189

摘要: 报道了一种新型Ag/Ag₃PO₄/g-C₃N₄三元复合光催化剂的制备及其半导体界面处的快速载流子分离所引起的光催化活性的显著增强效应。通过X射线衍射, 扫描电子显微镜, 紫外-可见吸收光谱以及光致发光光谱等就其晶体结构、形貌、组分、光学吸收以及载流子的快速分离行为进行了表征与分析。以罗丹明B作为模型化合物分子, 研究发现, 所制备的Ag/Ag₃PO₄/g-C₃N₄三元复合光催化剂在可见光照射下表现出比Ag₃PO₄以及Ag₃PO₄/g-C₃N₄二元催化剂更为优异的光催化活性。研究认为, Ag₃PO₄表面尺寸约为40 nm的Ag纳米粒子在可见光下受激所产生的等离子体表面共振效应以及Ag₃PO₄与g-C₃N₄界面处所形成的类似异质结构对所制备的Ag/Ag₃PO₄/g-C₃N₄三元复合光催化剂光催化活性的显著增强起到重要作用。

关键词: 银纳米粒子; 磷酸银; 石墨型氮化碳; 表面等离子共振; 异质结

收稿日期: 2013-07-26. 接受日期: 2013-09-10. 出版日期: 2014-01-20.

*通讯联系人. 电话: (025)84895871; 传真: (025)84895871; 电子信箱: shenkai84@nuaa.edu.cn

#通讯联系人. 电话: +966-3-8602351; 传真: +966-3-8604281; 电子信箱: magondal@kfupm.edu.sa

基金来源: 国家自然科学基金(51172044); 阿拉伯法赫德国王石油矿产大学-美国麻省理工学院国际合作基金(R15-CW-11, MIT11109, MIT11110).

本文的英文电子版由Elsevier出版社在ScienceDirect上出版(<http://www.sciencedirect.com/science/journal/18722067>).